# Absorption and Penetration of Left-Hand Polarized Waves Related to Polarization Reversal Causing Electron Cyclotron Resonance



doi: 10.1103/PhysRevE.74.016405

# Absorption and penetration of left-hand polarized waves related to polarization reversal causing electron cyclotron resonance

K. Takahashi,* T. Kaneko, and R. Hatakeyama
*Department of Electronic Engineering, Tohoku University, Sendai 980-8579, Japan*
(Received 7 February 2006; published 28 July 2006)

Propagation and absorption of electromagnetic waves with electron cyclotron resonance (ECR) frequency are investigated for the case of inhomogeneously magnetized plasmas, when the left-hand polarized wave (LHPW) is selectively launched. The LHPW with axisymmetric-azimuthal and second-order radial modes is absorbed near the ECR point at any radial position, which is caused by the polarization reversal to the right-hand polarized wave. On the other hand, it is clarified that the LHPW with fundamental radial mode penetrates the ECR point without polarization reversal. In addition, it is theoretically suggested that polarization reversal can partially occur in the plasma column for the case of nonaxisymmetric modes.

DOI: 10.1103/PhysRevE.74.016405 PACS number(s): 52.35.Hr, 52.40.Fd, 52.25.Mq

## I. INTRODUCTION

Propagation and absorptions of electromagnetic waves in magnetized plasmas have been investigated for a long time, because the waves embrace interesting physics and afford good possibilities of wide-range applications. Especially, electromagnetic waves with electron cyclotron resonance (ECR) frequency have attractive characteristics for realizing a thermonuclear fusion, as plasma sources for plasma processing, and so on. In the field of the thermonuclear fusion, ECR is indispensable for efficient electron heating [1] and the formation of local-confining potential structure in tandem-mirror devices [2,3]. On the other hand, ECR has been considered to be effective for the production of plasmas with high density, large diameter, lower electron temperature, and uniform density profile in the field of processing plasma [4–7]. It is obvious that wave propagation and absorption decide the heating efficiency and plasma characteristics produced.

In the past, many studies of the whistler wave were carried out for the case of weakly magnetized plasmas ($\omega_{pe}/\omega_{ce}>1$) [8–14] because the wave has right-handed polarization and is efficiently absorbed near the ECR point, where $\omega_{pe}$ and $\omega_{ce}$ are the electron plasma and cyclotron frequencies, respectively. On the other hand, investigations of wave propagation and absorption under the condition of $\omega_{pe}/\omega_{ce}<1$ have recently been carried out on purpose to produce uniform plasmas [15,16]. These experimental results showed that a left-hand polarized wave (LHPW), which is considered not to be related to ECR, is locally absorbed near the ECR point in inhomogeneously magnetized plasmas. In order to explain the unexpected absorption, a polarization reversal from the LHPW to a right-hand polarized wave (RHPW) was theoretically suggested for the case of $m=-1$ mode by including the effects of radial boundaries and finite electron temperature [17]. Here, $m$ is an azimuthal mode number and the authors of [17] insisted that the wave polarization is changed along the radial axis; namely, the polarization becomes right handed in some radial region. Although an experiment on polarization reversal was performed in an ECR discharge [15], it was difficult to obtain clear-cut experimental results because of the simultaneous realization of the purposes for both studying the wave propagation and producing the plasma. Therefore, we reported the experimental results for the case that the RHPW or LHPW with small amplitude is selectively launched in the steady-state plasma produced by a dc discharge [18–20]. In a previous paper, we reported that the damping region of the LHPW is more localized than that of the RHPW [18]. Then, this phenomenon is considered to be useful for more localized electron heating in high-temperature plasmas. However, the damping mechanisms of the LHPW near the ECR point have not been clarified, although radial boundaries have been supposed to exercise some effects on it. Besides, theoretical and numerical analyses are advanced for clarifying the effects of the boundaries in plasma waveguides [21–24]. Therefore, it is an important subject to unify the relationship between the effects of the boundary conditions and the unsettled problems, especially the unexpected absorption of the LHPW near the ECR point.

Based on the above-mentioned background, the purpose of the present work is to clarify the propagation and damping mechanisms of the LHPW near the ECR point from the viewpoint of the effects of the radial boundaries. We have already reported on the damping mechanism of the LHPW due to polarization reversal for the case of $m=0$ mode [25,26]. However, it was observed that a part of the launched LHPW is not absorbed, whose mechanism was not illuminated and has not been released so far. Thus, in this paper, we report the difference in the propagation mechanisms between LHPW's with an axisymmetric $m=0$ mode, one of which is absorbed near the ECR point and the other of which passes the ECR point without absorption. Furthermore, we theoretically discuss the characteristics of the polarization reversals for the case of axisymmetric $m=0$ and nonaxisymmetric $m=\pm 1$ modes. In Secs. II and III, an experimental setup and a dispersion theory are described. Experimental results about the axisymmetric mode are presented in Sec. IV, and the differences between the axisymmetric and nonaxisymmetric modes are discussed in Sec. V. Conclusions are given in Sec. VI.

*Electronic address: kazunori@ecei.tohoku.ac.jp

 

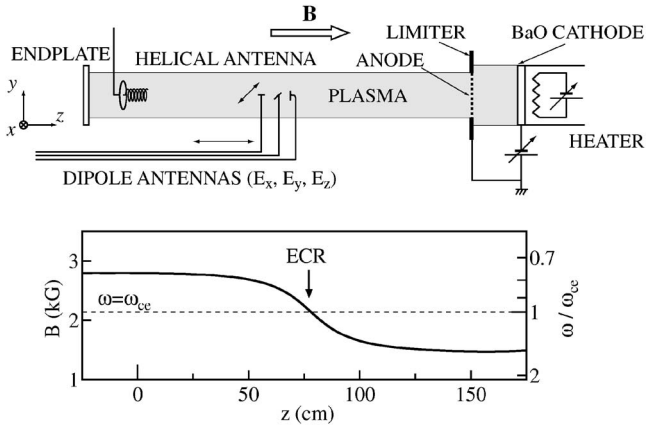


FIG. 1. Schematic of experimental setup and external static magnetic-field configuration.

## II. EXPERIMENTAL SETUP

Experiments are performed in the $Q_T$-Upgrade Machine of Tohoku University shown in the top of Fig. 1, which has a cylindrical vacuum chamber about 450 cm in length and 20.8 cm in inner diameter. An inhomogeneous magnetic field $B$ presented in the bottom of Fig. 1 is applied by two parties of solenoidal coils along the $z$ axis. Since the ECR magnetic-field strength for 6-GHz microwaves is 2.14 kG, the ECR point is located at $z=78$ cm. The plasma is produced by a dc discharge between an oxide cathode and a tungsten mesh anode in low-pressure argon gas (90 mPa). As the plasma column is terminated by a glass end plate, the electron velocity distribution becomes Maxwellian. The electron density and the temperature are measured by small Langmuir probes, and the operating electron density and temperature at the ECR point are fixed at $9\times10^{10}$ cm$^{-3}$ $(\omega_{pe}/\omega_{ce}<1)$ and 3 eV, respectively. The formation of a clear boundary between the plasma and peripheral vacuum layer is realized by using a limiter, which is located in front of the anode and has a diameter of 6 cm.

The small-amplitude LHPW (frequency $\omega/2\pi=6$ GHz, power 150 mW) is selectively launched into the plasma in the high-magnetic-field region by a helical antenna ($z=0$ cm). The antenna is designed to operate at $\omega/2\pi=6$ GHz in accordance with Ref. [27], where the diameter of the helix, axial length, number of turns, and diameter of the ground plane behind the helix are 1.6 cm, 12 cm, 10 turns, and 3.75 cm, respectively. We have already reported that the antenna selectively excites the LHPW [18]. We mention that the antenna excites transverse-electric- (TE-) field modes in the vacuum chamber when the plasma is not produced in the column. The launched LHPW propagates toward the ECR point satisfying the condition of $\omega/\omega_{ce}<1$. The wave patterns are obtained with an interference method by using a mixer through balanced dipole antennas with folded balun, which can receive each component of the wave electric field $E_x$, $E_y$, and $E_z$, respectively, and are terminated with 50 Ω lines. Here, the length of the dipole is selected to be 1.8 cm according to the fact that the antennas have the best sensitivity for the case of this length. In addition, the amplitude squares of each component of the electric field—i.e., $|E_x|^2$, $|E_y|^2$, and $|E_z|^2$—are measured with a power meter.

## III. DISPERSION THEORY

A dielectric tensor $\mathbf{K}$ in cold and uniform plasmas is given by

$$\frac{\omega^2}{c^2}\mathbf{K}=\begin{pmatrix}\kappa_1 & \kappa_2 & 0\\ -\kappa_2 & \kappa_1 & 0\\ 0 & 0 & \kappa_3\end{pmatrix}, \tag{1}$$

with $\kappa_1$, $\kappa_2$, and $\kappa_3$ defined by

$$\frac{c^2}{\omega^2}\kappa_1=1-\sum_j\frac{\omega_{pj}^2}{\omega^2-\omega_{cj}^2},$$

$$i\frac{c^2}{\omega^2}\kappa_2=\sum_j\frac{\epsilon_j\omega_{cj}\omega_{pj}^2}{\omega(\omega^2-\omega_{cj}^2)},$$

$$\frac{c^2}{\omega^2}\kappa_3=1-\sum_j\frac{\omega_{pj}^2}{\omega^2},$$

where $\omega_{pj}$, $\omega_{cj}$, and $\epsilon_j$ are the plasma frequency, the cyclotron frequency, and the sign of the charge for species $j$. The terms related to ion motions can be neglected in the case of $\omega\gg\omega_{pi}$, $\omega_{ci}$, where $\omega_{pi}$ and $\omega_{ci}$ are the ion plasma and cyclotron frequencies. A dispersion relation of electromagnetic waves in bounded plasmas is derived by using the Maxwell equations as [28]

$$(\gamma^2+\kappa_2^2+\gamma k_\perp^2)\kappa_3+k_\perp^2[\kappa_1(\gamma+k_\perp^2)-\kappa_2^2]=0, \tag{2}$$

where $\gamma\equiv k_\parallel^2-\kappa_1$ and $k_\parallel$ and $k_\perp$ are the wave numbers parallel and perpendicular to a static magnetic field $\mathbf{B}$, respectively. The electric fields are assumed to propagate toward the $z$ direction, so the wave fields with azimuthal mode number $m$ can be represented by

$$\mathbf{E}=\mathbf{E}(r)\exp[i(k_\parallel z+m\theta-\omega t)], \tag{3}$$

where the components of the electric-field vector $\mathbf{E}(r)$ are derived as

$$E_z(r)=\frac{\omega\kappa_1\beta A}{k_\parallel\kappa_2\kappa_3}J_m(k_\perp r), \tag{4}$$

$$E_r(r)=\frac{i\omega\delta A}{\kappa_2 k_\perp}J_m'(k_\perp r)-\frac{m\omega A}{rk_\perp^2}J_m(k_\perp r), \tag{5}$$

$$E_\theta(r)=-\frac{m\omega\delta A}{r\kappa_2 k_\perp^2}J_m(k_\perp r)-\frac{i\omega A}{k_\perp}J_m'(k_\perp r). \tag{6}$$

Here $\beta\equiv\gamma-\kappa_2^2/\kappa_1+k_\perp^2$, $\delta\equiv\gamma+k_\perp^2$, and $A$ and $J_m$ are an amplitude constant and Bessel function of order $m$, respectively. Here, $E_r$ and $E_\theta$ in cylindrical coordinates correspond to experimentally obtained $E_x$ and $E_y$ in rectangular coordinates. The perpendicular wave number $k_\perp$ is determined by radial boundary conditions when the radii of the plasma column

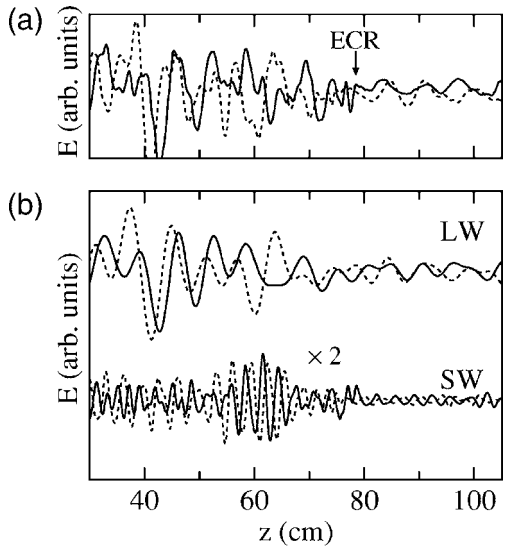


FIG. 2. (a) Interferometric wave patterns of $E_x$ (dashed line) and $E_y$ (solid line) observed at the radial center of the plasma column. (b) Long (LW) and short (SW) wavelength components decomposed from the wave patterns in Fig. 2(a) by using Fourier analysis.

and the vacuum chamber are comparable to the wavelength. Although the parallel wave number $k_\parallel$ is also affected by axial boundary conditions, we can neglect its effects because the parallel wavelength is much less than the axial length of the plasma column in our experimental configurations. Moreover, the effects of the inhomogeneous magnetic-field configuration should be included in the above-mentioned dispersion theory, which has already been described in Ref. [26].

It is well known that wave polarization plays important roles in cyclotron resonance phenomena. The above dispersion relation and electric-field components derive a polarization index $S$ as

$$S \equiv \frac{|E_r + iE_\theta|}{|E_r - iE_\theta|}. \tag{7}$$

Here, $0<S<1$ and $1<S<\infty$ represent right-handed and left-handed polarizations and $S=0$, $S=1$, and $S=\infty$ correspond to circularly right-handed, linear, and circularly left-handed polarizations, respectively. We mention that the wave polarization can become both right-handed and left-handed following Eq. (7), which is determined by Eqs. (5) and (6) derived from the solution of Eq. (2).

## IV. EXPERIMENTAL RESULTS

Figure 2(a) shows the interferometric wave patterns of $E_x$ (dashed line) and $E_y$ (solid line), where the solid arrow at $z=78$ cm represents the ECR point of 6-GHz microwaves. The observed wave patterns indicate the damping of the launched wave near the ECR point in spite of the selective launch of the LHPW, which has been considered not to be related to ECR. We have confirmed that the wave is not standing but traveling in the $z$ direction by shifting a phase of the received signal, which evidences that the dissipation of the wave near the ECR point is due to not a reflection but an absorption. Moreover, it is to be noted in Fig. 2(a) that the wave patterns include both the long (LW) and the short (SW) wavelength components and that a slight part of the LW penetrates the ECR point. The LW and SW are decomposed from the wave patterns in Fig. 2(a) by using Fourier analysis and presented in Fig. 2(b). Figure 2(b) shows that the LW damps and the SW grows around $z=60$ cm and that the wave patterns of $E_x$ in the LW and SW are shifted to the left and to the right of the wave patterns of $E_y$, respectively. From these phase differences between $E_x$ and $E_y$, the LW and SW are identified as LHPW and RHPW, respectively. Therefore, the observed wave patterns evidence that the LHPW damps and the RHPW grows around $z=60$ cm; i.e., polarization reversal from the LHPW to the RHPW occurs. As a result of the polarization reversal, the greater part of the launched LHPW is found to be absorbed near the ECR point, because the rotating direction of the wave electric field—i.e., polarization—is right-handed near the ECR point. The LHPW penetrating the ECR point is discussed later.

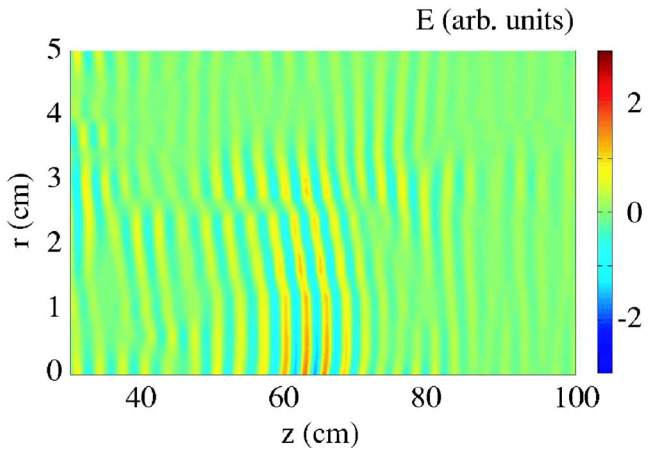


FIG. 3. (Color online) $r$-$z$ profile of the RHPW component decomposed from the interferometric wave patterns, which indicates that polarization reversal to the RHPW simultaneously occurs in the whole plasma column.

Figure 3 presents the $r$-$z$ profile of the electric field of the RHPW components decomposed from the observed wave patterns. Growth of the RHPW—i.e., the polarization reversal to the RHPW—is observed to take place at any radial position in the plasma column ($r \leqslant 3$cm). Moreover, the axial-polarization-reversal points are found to be homogeneously distributed in the radial direction, where the RHPW grows and has a maximum amplitude. Although the polarization reversal from the LHPW to the RHPW was theoretically reported for the case of $m=-1$ mode in the previous study, the polarization was predicted to remain left-handed along the axial axis at the plasma center in this theory [17]. The comparison of a theory for $m=\pm 1$ mode with our experimental results is discussed in Sec. V.

The radial profile of the axial component of the electric-field amplitude squares $|E_z|^2$ at $z=40$ cm is presented in Fig. 4(a) as a solid line for the identification of $m$ and $k_\perp$ by comparison with Eq. (4), which has a maximum power at the radial center and becomes almost zero in the peripheral

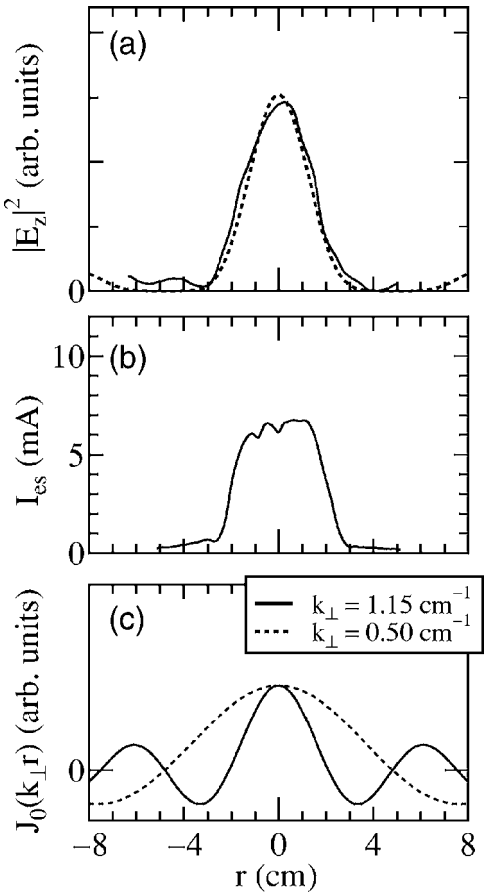


FIG. 4. (a) Radial profiles of electric-field amplitude squares $|E_z|^2$ (solid line) at $z=40$ cm together with the approximate curve (dashed line) given by the Bessel function of order zero, which is the superimposition of $J_0(0.50r)$ and $J_0(1.15r)$. (b) Radial profile of electron saturation current measured by the small Langmuir probe. (c) Calculated Bessel functions $J_0(0.50r)$ and $J_0(1.15r)$.

vacuum layer. Figure 4(b) denotes the radial profile of the electron saturation current $I_{es}$ measured by the Langmuir probe located at $z=40$ cm, which corresponds to the electron density. The electron density has a finite value even in the peripheral vacuum layer due to the radial diffusion. The radial profile of $|E_z|^2$ shown in Fig. 4(a) is attributed to the designed helical antenna, which excites the TE-field mode in the empty waveguide. The antenna characteristics originates the condition $E_z=0$ in the vacuum layer. In the plasma column, on the other hand, TE and transverse-magnetic- (TM-) field modes cannot independently exist except for some special cases. Therefore, $|E_z|^2$ is localized in the plasma column as presented in Fig. 4(a). The radial profile of $|E_z|^2$ of a certain mode in the plasma column can theoretically be represented by the Bessel function of order $m$ as shown in Eq. (4). The experimental profile of $|E_z|^2$ can be reproduced by the superimposition of $J_0(0.50r)$ and $J_0(1.15r)$ as a dashed line in Fig. 4(a). Thereby, two $m=0$ modes with $k_\perp=0.50$ and 1.15 cm$^{-1}$ are considered to be simultaneously excited in the plasma column by the helical antenna. Here, let us conjecture the radial position where $k_\perp$ is determined. The calculated Bessel functions $J_0(0.50r)$ and $J_0(1.15r)$ are plotted in Fig. 4(c) as dashed and solid lines, respectively. It is found that both $J_0(0.50r)$ and $J_0(1.15r)$ become zero at $|r| \simeq 4.8$ cm, where the electron density is almost zero as shown in Fig. 4(b). Therefore, $k_\perp$ is considered to be determined by the boundary condition $(E_z=0)$ at $r=\pm 4.8$ cm. Based on the above-mentioned consideration, it is identified that the modes with $k_\perp=0.50$ and 1.15 cm$^{-1}$ are $n=1$ and $n=2$ modes formed in the range of $|r|<4.8$ cm, where $n$ is the radial mode number.

The calculated dispersion relations of $n=2$ mode are presented in Fig. 5(a) as solid lines together with experimental ones of the LHPW (open square) with large amplitude in the upper region ($z<60$ cm) of the wave propagation and of the RHPW (open circle) near the ECR point (55 cm$<z<$78 cm), which are obtained from the decomposed wave patterns in Fig. 2(b). The experimental results of both the LHPW and RHPW are in good agreement with the calculated dispersion curve of the slow wave (bold line). The calculated polarization index $S$ corresponding to the dispersion relation in Fig. 5(a) is presented in Fig. 5(b). The calculated $S$ of the slow wave (bold line) shows that the wave polarizations are left-handed $(S>1)$ and right-handed $(S<1)$ in the range of $\omega/\omega_{ce}<0.85$ and $\omega/\omega_{ce}>0.85$, respectively. Thus, the observed polarization reversal to the RHPW is clarified to occur obeying the dispersion relation including the effects of the radial boundary between the plasma and the peripheral vacuum layer. We mentioned that a part of the LHPW can penetrate the ECR point without absorption as seen in Fig. 2. This residual LHPW cannot be explained by the dispersion relation of $n=2$ mode in Fig. 5(a). Then, the calculated dispersion relations of $n=1$ mode are compared with the experimental dispersion relation of the residual LHPW ($z>78$ cm), which are plotted in Fig. 5(c) as solid lines and solid squares, respectively. The experimental dispersion relation is in good agreement with the calculated curve of the fast wave (bold line). The polarization index of the fast wave, which is shown in Fig. 5(d) as a bold line, always designates the left-handed polarization $(S>1)$. Therefore, the LHPW of $n=1$ mode is found to pass through the ECR point, because polarization reversal to the RHPW never occurs. In our experimental configuration, the value of $\omega/\omega_{ce}$ at the position of the microwave exciter—i.e., the helical antenna—is about 0.75 as shown in Fig. 1. Since the helical antenna generates the LHPW and the waves with left-handed polarization at $\omega/\omega_{ce}\simeq 0.75$ are only the fast wave for $n=1$ and the slow wave for $n=2$ in the dispersion relation in Fig. 5, the excited $n=1$ and $n=2$ modes result in the formation of the fast and slow waves, respectively.

## V. DISCUSSION

Polarization reversal due to a radial boundary is observed to occur at any radial position in the plasma column in our experiments (see Fig. 3). Since Ganguli *et al.* suggested that polarization reversal can occur only around the plasma edge for the case of $m=\pm 1$ modes [17], the polarization reversal in our experiments has characteristics different from the one for $m=\pm 1$ modes. In this section, we discuss the polarization-reversal characteristics in our experiments and

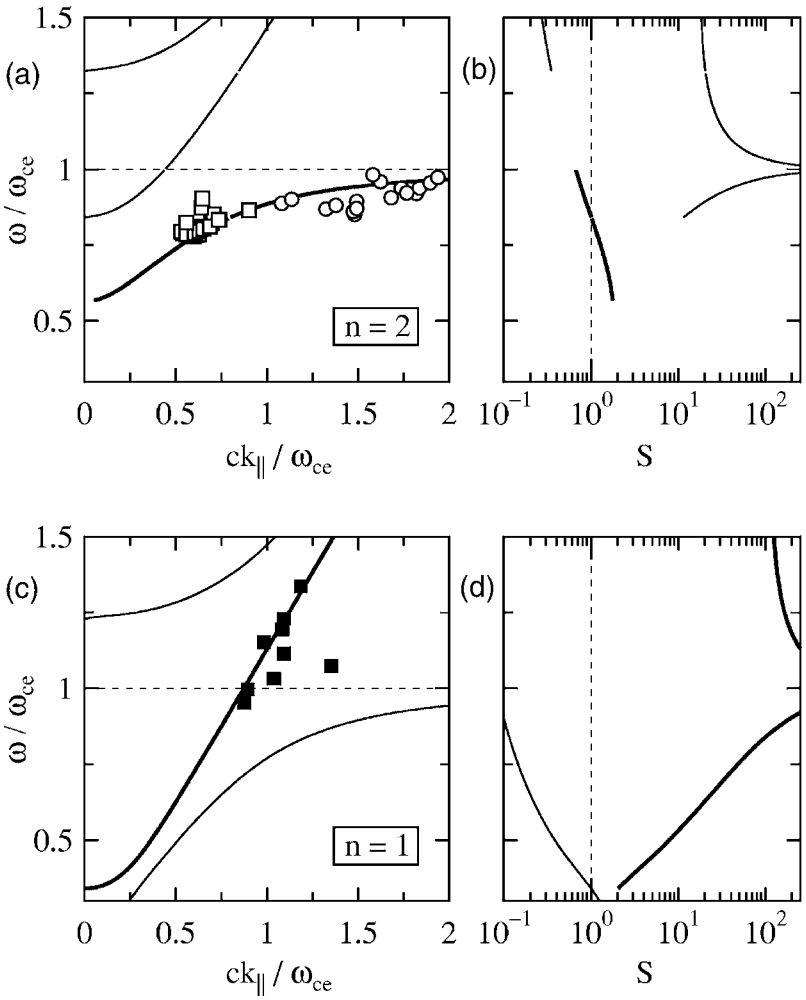


FIG. 5. Calculated dispersion relations for (a) $n=2$ and (c) $n=1$ together with the experimental dispersion relation of the LHPW (open square) in the upper region, the RHPW (open circle) near the ECR point, and the LHPW (solid square) penetrating the ECR point. (b), (d) Calculated polarization indexes $S$ corresponding to the dispersion relations in (a) and (c).

compare them with the polarization reversal for $m=\pm 1$ modes by using the dispersion relation of Eq. (2).

So as to interpret the result in Fig. 3, the radial profiles of the polarization index $S$ of the slow wave for $m=0$ and $n=2$ modes are calculated with $\omega/\omega_{ce}$ as a parameter, where $\omega/\omega_{ce}$ corresponds to the axial position $z$. The calculated results for the case of $\omega/\omega_{ce}=0.72$, 0.86, and 0.97 are shown in Fig. 6. For each $\omega/\omega_{ce}$, the polarization index $S$ is found to be homogeneously distributed along the radial axis. The polarization is left-handed at any radial position for the case of $\omega/\omega_{ce}=0.72$. In the cases of $\omega/\omega_{ce}=0.86$ and 0.97, on the other hand, it is noted that the polarization at any radial position simultaneously becomes right-handed. The calculated results can explain the observed phenomenon in Fig. 3, which means that polarization reversal from the LHPW to the RHPW simultaneously occurs at any radial position.

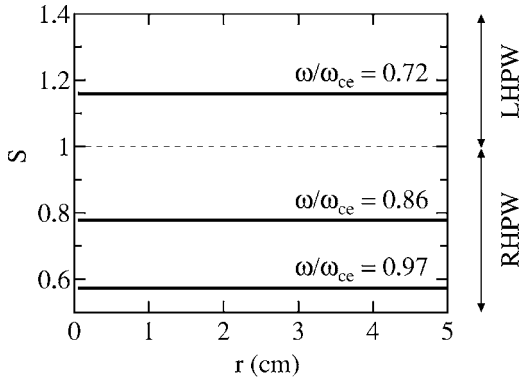


FIG. 6. Calculated radial profile of polarization index $S$ with $\omega/\omega_{ce}$—i.e., magnetic-field strength $B$—as a parameter for the case of the $m=0$ mode.

Figure 7 shows the calculated radial profiles of the polarization index $S$ for the case of the $m=+1$ mode with $\omega/\omega_{ce}$ as a parameter, where the value of $k_\perp$ is the same as in Fig. 6. The shaded regions describe $S<1$; i.e., the wave polarization is right-handed. Figure 7 indicates that the wave polarization around the radial center of the plasma column is right-handed under all conditions for $m=+1$. It is confirmed that the wave polarization varies along the radial axis for any $\omega/\omega_{ce}$; e.g., the polarizations are right- and left-handed in the range of $r=0-1.5$ cm and $r=1.5-3.5$ cm for $\omega/\omega_{ce}=0.72$, respectively. The result is essentially the same as the past reports by Ganguli *et al.*[17]. Moreover, our attention is focused on its axial variation depending on the magnetic-field strength. As $\omega/\omega_{ce}$ is closer to unity, it is found that the shaded region is extended. That is to say, the wave polarization axially varies around $r\simeq 1.8$ and 3.5 cm; namely, polarization reversal from the LHPW to the RHPW can theoretically occur around these positions for the case of the $m=+1$ mode.

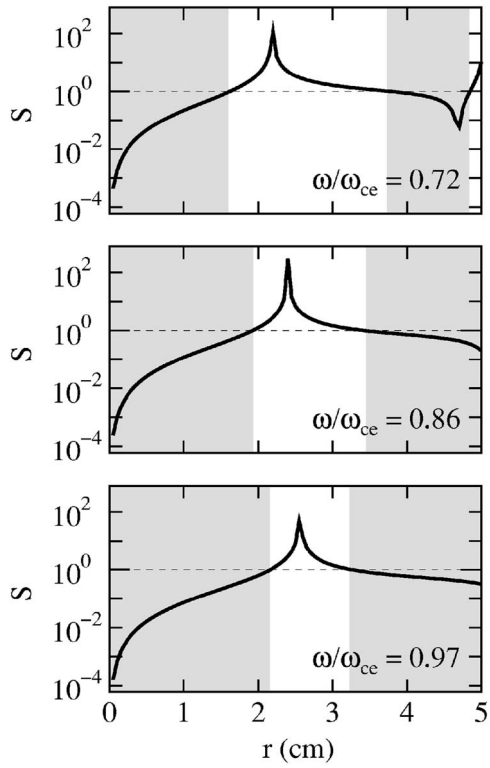


FIG. 7. Calculated radial profiles of the polarization index $S$ with $\omega/\omega_{ce}$ as a parameter for the case of the $m=+1$ mode.

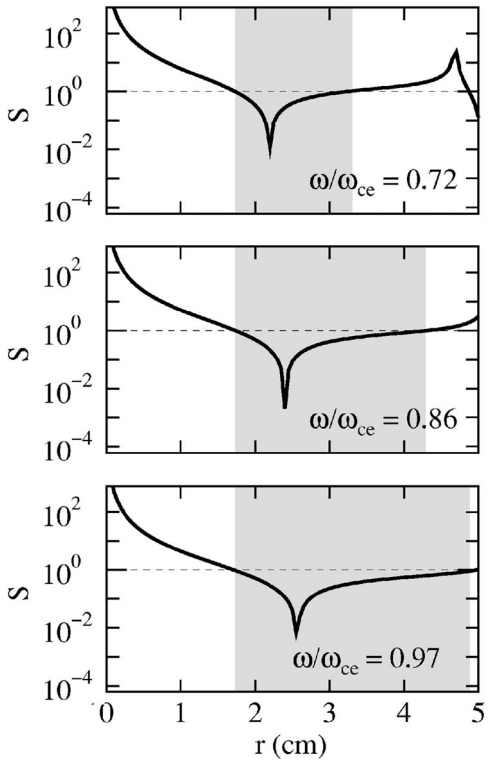


FIG. 8. Calculated radial profiles of the polarization index $S$ with $\omega/\omega_{ce}$ as a parameter for the case of the $m=-1$ mode.

Next, the calculated radial profiles of the polarization index $S$ with $\omega/\omega_{ce}$ as a parameter for the case of $m=-1$ mode are presented in Fig. 8. The regions where the wave polarization is right-handed are also shaded. Although the wave polarization around the radial center of the plasma column is left-handed for any $\omega/\omega_{ce}$, the polarization turns out to be right-handed at some radial positions. It is noticed that the region where the polarization is right-handed widens as the wave approaches to the ECR point. Therefore, the wave polarization for $m=-1$ mode also axially varies—e.g., $r \simeq 3.5$ cm.

After all, polarization reversal from the LHPW to the RHPW occurs at any radial position since the launched LHPW has the $m=0$ mode in our experiments. According to our theoretical analyses for the cases of $m=0$ and $\pm 1$ modes, it is expected that the characteristics of polarization reversal from the LHPW to the RHPW depend on the excited azimuthal mode.

## VI. CONCLUSION

The propagation and absorption mechanisms of high-frequency electromagnetic waves near the electron cyclotron resonance point are experimentally and theoretically investigated for the case of an inhomogeneously magnetized plasma, when the left-hand polarized wave is selectively launched in the high-magnetic-field region by the helical antenna. Our experimental results prove the polarization reversal from the LHPW to the right-hand polarized wave at any radial position in the plasma column for the case of $m=0$ mode and the resultant absorption of the launched LHPW near the ECR point. The observed polarization reversal can well be explained by including the effects of the radial boundary between the plasma and peripheral vacuum layer. The residual LHPW in the low-magnetic-field region after the ECR point is found to be a fast wave, which is not converted to the RHPW. After all, the LHPW with the fundamental radial mode ($n=1$) passes through the ECR point without the polarization reversal, and the LHPW with the second radial mode ($n=2$) is absorbed near the ECR point due to the polarization reversal. In addition, our analyses imply the existence of polarization reversal in the peripheral region of the plasma for the case of $m=\pm 1$ modes. As the wave absorption profile is affected by the wave polarization profile, our experimental and calculated results could play important roles in the control of the electron heating and acceleration profile.

## ACKNOWLEDGMENTS

The authors are indebted to H. Ishida for his technical assistance. We also express our gratitude to Professor K. Sawaya for his useful comments. This work was supported by a Grant-in-Aid for Scientific Research from the Ministry of Education, Culture, Sports, Science and Technology, Japan. The work was also supported by the Japan Society for the Promotion of Science for Young Scientists.

[1] Y. Ikeda, S. Ide, T. Suzuki, A. Kasugai, K. Takahashi, K. Kajiwara, A. Isayama, T. Oikawa, K. Hamamatsu, Y. Kamada, T. Fujita, K. Sakamoto, S. Moriyama, M. Seki, R. Yoshino, T. Imai, K. Ushigusa, T. Fujii, and JT-60 Team, Nucl. Fusion **42**, 375 (2002).
[2] T. Kaneko, R. Hatakeyama, and N. Sato, Phys. Rev. Lett. **80**, 2602 (1998).
[3] T. Cho, M. Yoshida, J. Kohagura, M. Hirata, T. Numakura, H. Higaki, H. Hojo, M. Ichimura, K. Ishii, K. M. Islam, A. Itakura, I. Katanuma, Y. Nakashima, T. Saito, Y. Tatematsu, M. Yoshikawa, Y. Kojima, S. Tokioka, N. Yokoyama, Y. Tomii, T. Imai, V. P. Pastukhov, S. Miyoshi, and Gamma 10 Group, Phys. Rev. Lett. **94**, 085002 (2005).
[4] Y. Ueda, M. Tanaka, S. Shinohara, and Y. Kawai, Rev. Sci. Instrum. **66**, 5423 (1995).
[5] T. Ono, S. Hiyama, Y. Nakagawa, S. Iizuka, and N. Sato, Plasma Sources Sci. Technol. **5**, 293 (1996).
[6] W. Miyazawa, S. Tada, K. Ito, H. Saito, S. Den, Y. Hayashi, Y. Okamoto, and Y. Sakamoto, Plasma Sources Sci. Technol. **5**, 265 (1996).
[7] R. D. Tarey, R. K. Jarwal, A. Ganguli, and M. K. Akhtar, Plasma Sources Sci. Technol. **6**, 189 (1997).
[8] G. Lisitano, M. Fontanesi, and S. Bernabei, Phys. Rev. Lett. **26**, 747 (1971).
[9] J. Musil and F. Zacek, Plasma Phys. **13**, 471 (1971).
[10] B. McVey and J. Scharer, Phys. Rev. Lett. **31**, 14 (1973).
[11] R. L. Stenzel, Phys. Rev. Lett. **35**, 574 (1975).
[12] R. L. Stenzel, Phys. Fluids **19**, 857 (1976).
[13] K. Ohkubo and S. Tanaka, J. Phys. Soc. Jpn. **41**, 254 (1976).
[14] H. Sugai, K. Ido, H. Niki, S. Takeda, and K. Mima, J. Phys. Soc. Jpn. **46**, 1647 (1979).
[15] A. Ganguli, M. K. Akhtar, R. D. Tarey, and R. K. Jarwal, Phys. Lett. A **250**, 137 (1998).
[16] Y. Ueda, H. Muta, and Y. Kawai, Appl. Phys. Lett. **74**, 1972 (1999).
[17] A. Ganguli, M. K. Akhtar, and R. D. Tarey, Phys. Plasmas **5**, 1178 (1998).
[18] T. Kaneko, H. Murai, R. Hatakeyama, and N. Sato, Phys. Plasmas **8**, 1455 (2001).
[19] K. Takahashi, T. Kaneko, and R. Hatakeyama, Trans. Fusion Sci. Technol. **43**, 95 (2003).
[20] K. Takahashi, T. Kaneko, and R. Hatakeyama, J. Plasma Fusion Res. **79**, 447 (2003).
[21] B. Maraghechi, J. E. Willett, H. Mehdian, and Y. Aktas, Phys. Plasmas **1**, 3181 (1994).
[22] S. Mirzanejhad and B. Maraghechi, Phys. Plasmas **5**, 4070 (1998).
[23] B. Maraghechi, B. Farrokhi, and J. E. Willett, Phys. Plasmas **6**, 3778 (1999).
[24] L. Shenggang, Y. Yang, M. Jie, and D. M. Manos, Phys. Rev. E **65**, 036411 (2002).
[25] K. Takahashi, T. Kaneko, and R. Hatakeyama, Phys. Rev. Lett. **94**, 215001 (2005).
[26] K. Takahashi, T. Kaneko, and R. Hatakeyama, Phys. Plasmas **12**, 102107 (2005).
[27] J. D. Kraus, *Antennas* (McGraw-Hill, New York, 1950).
[28] D. G. Swanson, *Plasma Waves*, 2nd ed. (Institute of Physics Publishing, Bristol, 2003).